Study on CO_2 Recovery Systems by Pressure Swing Adsorption under High Pressure Condition

Koga, Tsukasa
Graduate School of Engineering, Kyushu University

Matsukuma, Yosuke
Faculty of Engineering, Kyushu University

Inoue, Gen
Faculty of Engineering, Kyushu University

Minemoto, Masaki
Faculty of Engineering, Kyushu University

出版情報：Journal of Novel Carbon Resource Sciences. 3, pp.6-10, 2011-02. Kyushu University G-COE program "Novel Carbon Resource Sciences" secretariat
バージョン：
権利関係：

Kyushu University Global COE Program
Journal of Novel Carbon Resource Sciences, Vol. 3, pp. 6-10, Feb. 2011

Study on CO_2 Recovery Systems by Pressure Swing Adsorption under High Pressure Conditions

Tsukasa Koga[*1], Yosuke Matsukuma[*2], Gen Inoue[*2], Masaki Minemoto[*2]
[*1]Graduate School of Engineering, Kyushu University
[*2]Faculty of Engineering, Kyushu University

(Received November 12, 2010; accepted December 28, 2010)

The numerical simulations for adsorption and desorption of CO_2 under high pressure conditions are conducted to predict distributions of CO_2 concentration, gas temperature, adsorbed amount of CO_2, etc. in the adsorption tower as a function of decompression time. The decompression time, which is the period to decrease pressure in desorption process, changes the performance of the system. We seek the optimum decompression time to minimize the thermal energy loss in the range for 10 to 150s. As a result, it is revealed that the optimum decompression time is about 40s and the thermal energy loss is about 250 [kJ/kg-CO_2].

1. Introduction

Since coal is inexpensive and abounded in the world compared to oil and natural gas, coal fired power generation system, especially integrated coal gasification combined cycle (IGCC) system, has been focused as one of the promising power generation system[1]. In the IGCC, electricity is generated by both gas turbine and steam turbine. It is therefore more efficient than traditional pulverized coal combustion system. However, amount of CO_2 emission from coal is more than these of oil and natural gas. CO_2 recovery from exhaust gas of generating power plant is required from the viewpoint of preventing global warming. Figure 1 shows a proposed flow diagram of IGCC with CO_2 recovery system. In gasification furnace, coal is gasified with oxygen as gasifying agent. Main compositions of gasification gas are CO, H_2, CO_2 and H_2O. Next, chemical reaction of H_2O and CO produces H_2 and CO_2 in shift reactor. After sulfur removal process, CO_2 is removed by pressure swing adsorption (PSA) system. Here, PSA is an adsorption method utilizing change of the adsorption amount according to pressure. Details of PSA are illustrated later. Fuel gas, mainly comprised of H_2, is combusted with air in gas turbine combustor and electricity is generated by gas turbine. In heat recovery steam generator, steam is generated by heat recovered from the combustor and gasification furnace. And then, electricity is generated by steam turbine. Stack gas from this system is much cleaner than that from ordinary thermal power generation system. In the proposed system, the PSA system would be useful for CO_2 recovery because the operating pressure of IGCC is about 30 atm and this pressure is high enough to adsorb the CO_2. However, the optimum size and operating conditions for the PSA are still unknown. In this study, we conduct numerical simulations for adsorption and desorption of CO_2 by the PSA to obtain the optimum decompression time, which is the time required to reduce the pressure and one of the capital operating conditions.

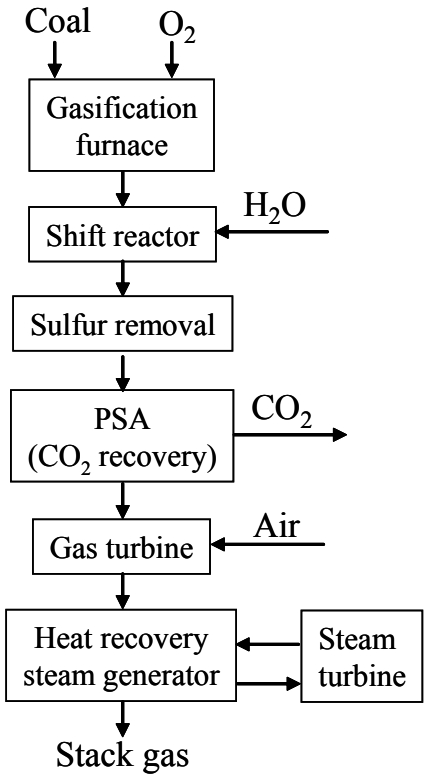

Fig. 1 Flow diagram of IGCC with CO_2 recovery system.

2. Simulation method

In PSA, mass and heat are transferred between the gas and adsorbent during each process of adsorption and desorption. So the one-dimensional simulations for adsorption and desorption of CO_2 are conducted to predict distributions of CO_2 concentration, gas temperature, honeycomb temperature, flow velocity, and adsorbed amount of CO_2 in the adsorption tower.

The basic equations represent (1) mass balance, (2) gas velocity, (3) mass transfer rate, (4) heat balance in the fluid, (5) heat balance in the adsorbent, and adsorption equilibrium obtained by our experiment[2].

$$\rho_m \frac{\partial q}{\partial t} + \frac{\partial (uC)}{\partial z} = 0 \tag{1}$$

$$\rho_C \frac{\partial u}{\partial z} = -k_F \cdot a(C - C^*) \times \frac{273.2}{T_g} \times \frac{p}{1.0} \tag{2}$$

$$\rho_m \frac{\partial q}{\partial t} = k_F \cdot a(C - C^*) \times \frac{273.2}{T_g} \times \frac{p}{1.0} \tag{3}$$

$$\left\{(\lambda_{gC} ux + \lambda_{gH} u(1-x)\right\} \frac{\partial T_g}{\partial z} = h \cdot a(T_m - T_g) \tag{4}$$

$$\rho_m \lambda_m \frac{\partial T_m}{\partial t} + \rho_m \lambda_C q \frac{\partial T_m}{\partial t} = \rho_m Q_{ad} \frac{\partial q}{\partial t} - h \cdot a(T_m - T_g) + \rho_m \lambda_C \frac{\partial q}{\partial t}\left(T_g - T_m\right) \tag{5}$$

The following assumptions were made.

1. The temperature, concentration and gas velocity in the radial direction are neglected.
2. The heat loss is neglected.
3. The diffusion of mass and heat is neglected.
4. The adsorption equilibrium can be shown with Langmuir's adsorption isotherm.
5. CO_2 is the only gas adsorbed.

Figure 2 shows diagram of adsorption and desorption process. In the adsorption process, H_2 and CO_2 gas enter from the left side with constant gas velocity u, and CO_2 is adsorbed by adsorbent under the pressure of 30 atm. When concentration of CO_2 gas at outlet reaches 20 %, the adsorption process is terminated. In the desorption process, pure CO_2 flows from right to left and CO_2 is desorbed under the pressure of 2 atm. When gas velocity of outlet gas becomes less than 1.5 times of inlet gas, we judge desorption is enough and the desorption process is terminated. At the start of the desorption process, the pressure is gradually reduced from 30 atm to 2 atm at a constant rate. We define the period required to reduce the pressure from 30 to 2 atm the decompression time. For example, Figure 3 shows time variations of pressure in the desorption process. The decompression time is 40s and 150s. For reference, the dotted line shows partial pressure of CO_2 in the adsorption process. A size of adsorption tower and operating conditions are listed in Table 1. A set of adsorption and desorption process is repeated until the system settled to their steady states.

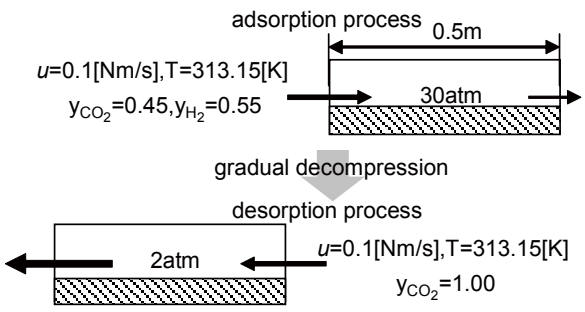

Fig. 2 Diagram of adsorption and desorption cycle.

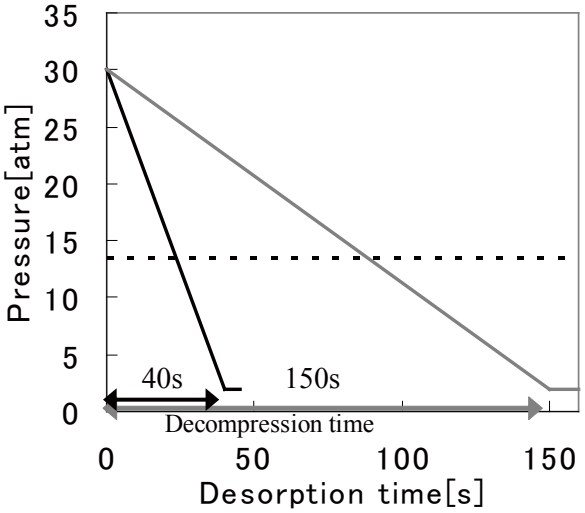

Fig. 3 Time variations of pressure in desorption process.

Table 1 Size and operating conditions

Size		
Height	0.5 m	
Hydraulic diameter	3.89×10^{-3} m	
Aperture ratio	0.419	
Effective surface area	745.0 m^2/m^3	
Operating conditions		
	Adsorption	Desorption
Velocity of inlet gas	0.1 Nm/s	0.1 Nm/s
Temperature of inlet gas	313.15 K	313.15 K
Concentration of inlet gas	CO_2 : 45% H_2 : 55%[1]	CO_2 :100%
Pressure	30 atm	2 atm

3. Simulation results

3.1 Distributions of CO_2 adsorbed amount in the adsorption tower

Figure 4 compares distributions of CO_2 adsorbed amount at the end of desorption process between 40s and 150s in decompression time. They are not steady state, but first cycle. Obvious difference of CO_2 adsorbed amount distribution appeared near inlet and outlet of tower. At

the start of desorption process, the pressure is higher than the partial pressure of CO_2 in the adsorption process as dotted line in Fig.3. Despite the desorption process, CO_2 adsorption still carried on until pressure decreased under the partial pressure. Figure 3 also illustrates that the longer the decompression time is, the longer time until pressure decreases under the partial pressure is required. Therefore, as the decompression time is longer, more CO_2 is adsorbed near the inlet (at Height=0.5). On the other hand, amount of CO_2 near the outlet (at Height=0) of the longer decompression time was less than that of the shorter decompression time, because increase of decompression time causes increase of desorption time. These are the reasons why distributions of CO_2 adsorbed amount were different depending on the decompression time.

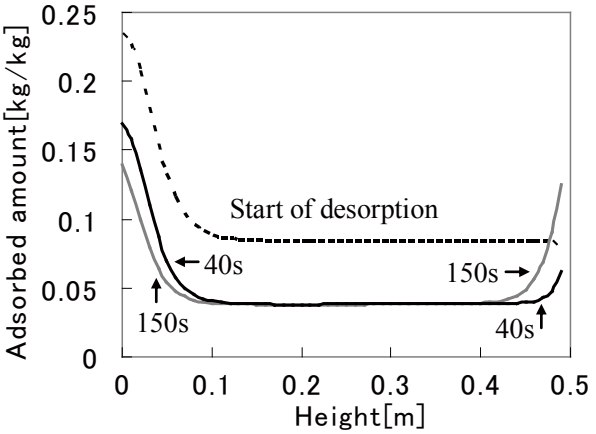

Fig. 4 Distributions of CO_2 adsorbed amount at the end of first desorption process.

The distribution changes as the cycles of adsorption and desorption are repeated, and the difference of distributions becomes more clear. Figure 5 and Figure 6 show the distributions of CO_2 adsorbed amount at the decompression time 40s and 150s, respectively. These figures indicate that a part of adsorbed CO_2 still remained in the adsorbent when the desorption process ends and the residual amount increased as the cycle repeats. Figure 7 shows CO_2 adsorbed amount in adsorption process after it becomes steady states (decompression time is 40s). Figure 7 and Figure 5 illustrate that adsorbed amount between adsorption process (shaded region in Fig.7) and desorbed amount between desorption process were almost equal. The shaded region in Fig.7 is the amount of CO_2 recovered by adsorbent between a cycle of adsorption and desorption process. It is defined as the recovery amount Q [kg/m^2] and calculated from Eq. (6).

$$Q = \int \left(u_{in} \cdot C_{in} - u_{out} \cdot C_{out} \right) dt \tag{6}$$

Figure 8 shows the recovery amount as a function of decompression time. From this figure, it was found that decompression time affected recovery amount. The difference between the maximum value at 40s and minimum value at 90s was about 20 %.

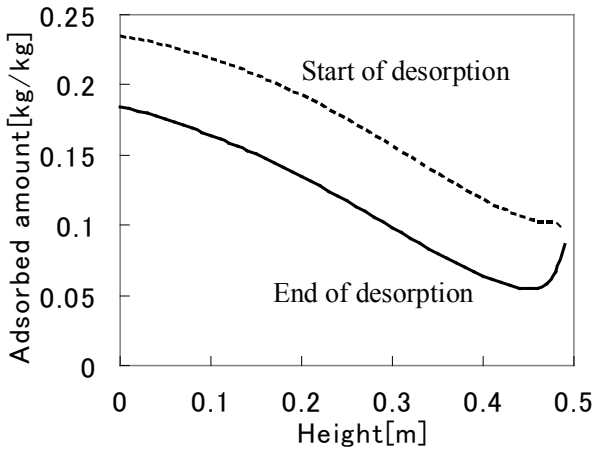

Fig. 5 Distributions of CO_2 adsorbed amount at decompression time of 40s.

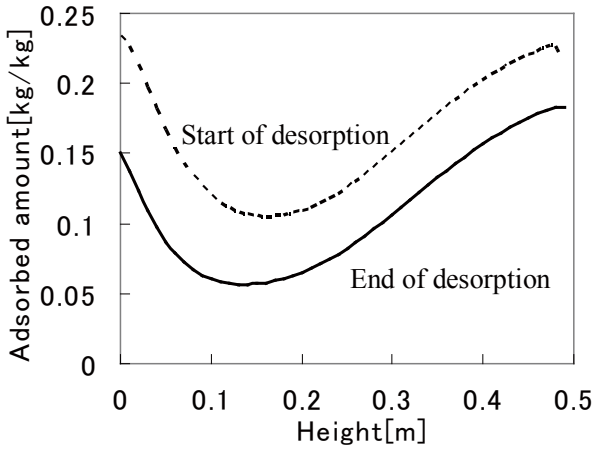

Fig. 6 Distributions of CO_2 adsorbed amount at decompression time of 150s.

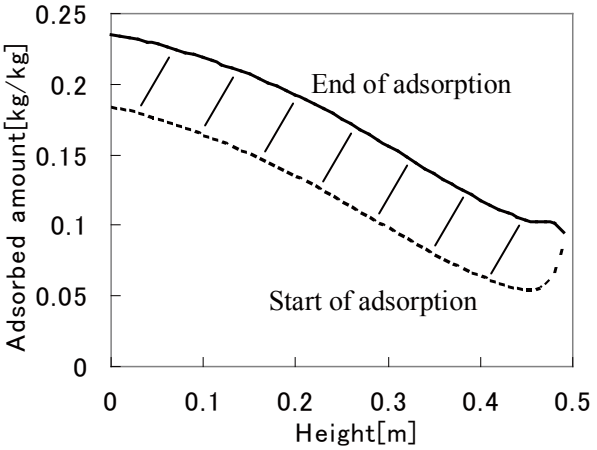

Fig. 7 Distributions of CO_2 adsorbed amount in adsorption process.

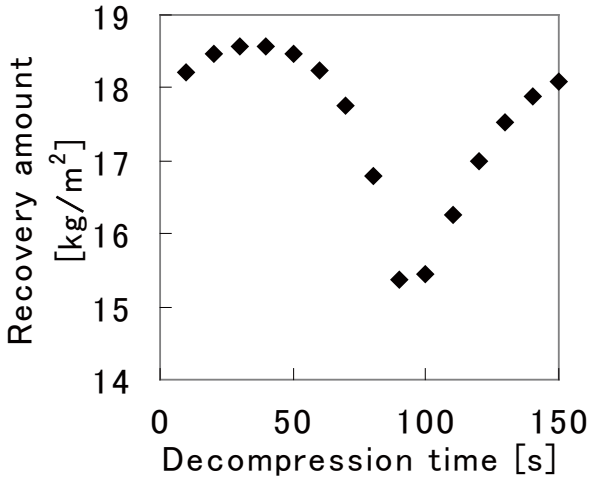

Fig. 8 Recovery amount and decompression time.

3.2 Performance analysis

In order to find the optimum decompression time, we define recovery rate, recovery speed and thermal energy loss. The recovery rate η [%] is defined by Eq. (7) as the rate of the amount of CO_2 recovered by adsorbent to the total amount of CO_2 in the inlet gas.

$$\eta = \frac{\int (u_{in} \cdot C_{in} - u_{out} \cdot C_{out}) dt}{\int u_{in} \cdot C_{in} dt} \times 100 \qquad (7)$$

Figure 9 shows the calculated recovery rate as a function of decompression time. From this figure, it is shown that the recovery rate was larger than 85 % in all the decompression times, and took the minimum value at the decompression time of 90s in this study's conditions.

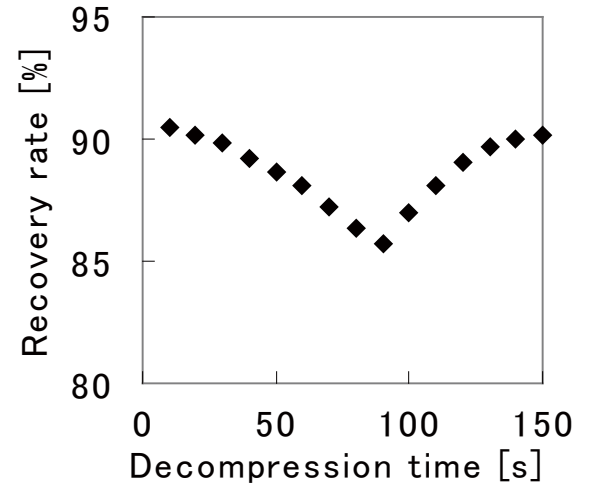

Fig. 9 Recovery rate and decompression time.

The recovery speed U [kg/m^2/h] is defined as the amount of CO_2 removed per unit time calculated from Eq. (8).

$$U = \frac{3600 \times \int (u_{in} \cdot C_{in} - u_{out} \cdot C_{out}) dt}{t_{ad} + t_{de}} \qquad (8)$$

Figure 10 shows the recovery speed as a function of decompression time. The recovery speed decreased with the decompression time, and the decreasing slope became low after decompression time of 90s. Decrease of the recovery speed can be greatly related to the fact that increase of decompression time causes increase of desorption time.

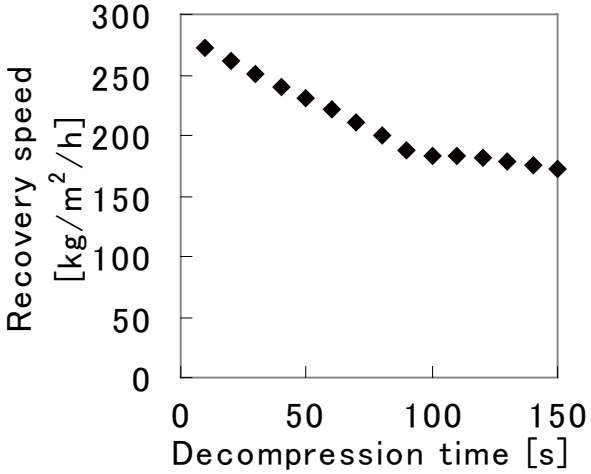

Fig. 10 Recovery speed and decompression time.

Thermal energy loss E [kJ/kg-CO_2] is defined as the lost thermal energy to remove 1 kg of CO_2 calculated from Eq. (9).

$$E = \frac{\int (\lambda_c \cdot u_{in} \cdot T_{g,in} - \lambda_c \cdot u_{out} \cdot T_{g,out}) dt}{\int (u_{in} \cdot C_{in} - u_{out} \cdot C_{out}) dt} \qquad (9)$$

Figure 11 shows change of thermal energy loss with decompression time. As the decompression time increased, the thermal energy loss decreased. It had the lowest value of 250 [kJ/kg-CO_2] at decompression time of 40s. Then, as the decompression time increased, the thermal energy loss increased. And, the highest value is about 300 [kJ/kg-CO_2]. Since the required energy to recover unit CO_2 is around 3000 [kJ/kg-CO_2] by existing adsorption and absorption system, the proposed system has possibilities to significantly reduce the required energy.

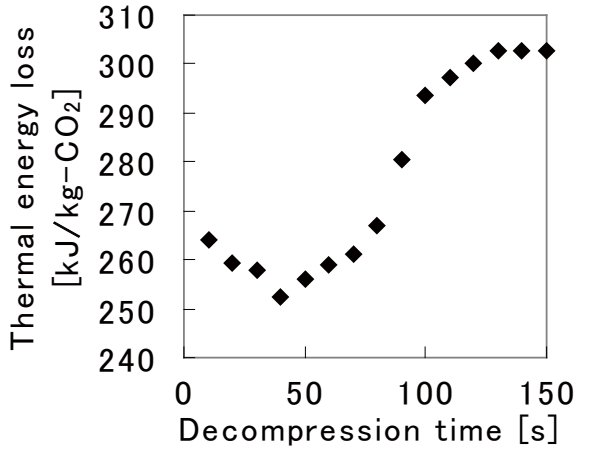

Fig. 11 Thermal energy loss and decompression time.

4. Conclusion

In this study, numerical simulations for adsorption and desorption of CO_2 by the PSA were conducted to obtain the optimum operating conditions. It was shown that the difference of decompression time influences the performance of PSA system. Thermal energy loss of PSA system might be much smaller than that of the other adsorption and absorption method under ordinary pressure (about 3000 [kJ/kg-CO_2]).

References

1) U.S. Department of Energy, National Energy Tecnology Laboratory, *Cost and Performance Baseline for Fossil Energy Plants*, *Volume 1: Bituminous Coal and Natural Gas to Electricity*, Pittsburgh, PA (2007).
2) Y. Matsukuma, Y. Matsushita, H. Kakigami, G. Inoue, M. Minemoto, A. Yasutake and N. Oka, *Kagaku Kogaku Ronbunshu*, **32**(2), 138 (2006).

Nomenclature

a	effective surface area	[m^2/m^3]
C	concentration of CO_2	[kg/Nm^3]
E	thermal energy loss	[kJ/kg]
h	heat transfer coefficient	[$W/(m^2 \cdot K)$]
k_F	mass transfer coefficient	[m/s]
p	pressure	[atm]
Q	recovery amount	[kg/m^2]
Q_{ad}	adsorption heat	[J/kg]
q	adsorbed amount	[kg/kg]
T	temperature	[K]
t	time	[s]
U	recovery speed	[$kg/(m^2 \cdot h)$]
u	gas velocity	[Nm/s]
x	mole fraction of CO_2	[-]
z	tower height	[m]

Greek letters

η	recovery rate	[-]
λ	specific heat	[$J/(kg \cdot K)$]
λ_g	gas specific heat	[$J/(m^3 \cdot K)$]
ρ_g	gas density	[kg/Nm^3]
ρ_m	adsorbent density	[kg/m^3]

Subscript

ad	adsorption process
C	CO_2
de	desorption process
g	gas
H	H_2
in	inlet of adsorption process
m	adsorbent
out	outlet of adsorption process
*	equilibrium